

Efficient Nonlinear Precoding for Massive MU-MIMO Downlink Systems with 1-Bit DACs

Lei Chu, *Student Member, IEEE*, Fei Wen, *Member, IEEE*, Lily Li, *Student Member, IEEE*, and Robert Qiu, *Fellow, IEEE*

Abstract—The power consumption of digital-to-analog converters (DACs) constitutes a significant proportion of the total power consumption in a massive multiuser multiple-input multiple-output (MU-MIMO) base station (BS). Using 1-bit DACs can significantly reduce the power consumption. This paper addresses the precoding problem for the massive narrow-band MU-MIMO downlink system equipped with 1-bit DACs at each BS. In such a system, the precoding problem plays a central role as the precoded symbols are affected by extra distortion introduced by 1-bit DACs. In this paper, we develop a highly-efficient nonlinear precoding algorithm based on the alternative direction method framework. Unlike the classic algorithms, such as the semidefinite relaxation (SDR) and squared-infinity norm Douglas-Rachford splitting (SQUID) algorithms, which solve convex relaxed versions of the original precoding problem, the new algorithm solves the original nonconvex problem directly. The new algorithm is guaranteed to globally converge under some mild conditions. A sufficient condition for its convergence has been derived. Experimental results in various conditions demonstrated that, the new algorithm can achieve state-of-the-art performance comparable to the SDR algorithm, while being much more efficient (e.g., more than 300 times faster than the SDR algorithm).

Index Terms—Massive multi-user multiple-input multiple-output, 1-bit digital-to-analog converter, nonlinear quantized precoder, alternative direction method, nonconvex optimization.

I. INTRODUCTION

IN recent years, there has been an increasing research attention in MU-MIMO systems, in which a base station (BS) is equipped with a large number of antennas, simultaneously serving many users terminals (UTs) in the same frequency band [1], [2]. Scaling up the number of the transmit antennas will lead to much more degrees of freedom available for each UT, and result in higher data rate and improved radiated energy efficiency. These benefits can be attained by simple linear processing such as maximum ratio transmission (MRT), zero-forcing (ZF) or water filling (WF) on the downlink [3], [4]. Accordingly, massive MU-MIMO is foreseen as a promising technology for 5G cellular systems. In order to make full use of the favorable properties that massive MU-MIMO can offer,

one needs to pay attention to the related disadvantage caused by the deployment of a large number of BS antennas. For example, the hardware cost and energy consumption grow linearly with the increase in the number of antennas, and exponentially with the increase in the number of quantization bits [5], [6]. In this paper, we consider 1-bit digital-to-analog converters (DACs) for massive MU-MIMO systems, which have the capability of dramatically reducing the hardware cost and energy consumption.

A. Related Works

The literature on quantized downlink wireless communication systems can be generally split into two categories, linear analysis and nonlinear analysis. The linear analysis derives its name by taking the advantages of the well-known Bussgang theorem [7], with which one can decompose the nonlinear quantized signal output into a linear function of the input to the quantizers and an uncorrelated distortion term [8]–[10]. Using proper signal processing techniques, the quantized precoding problem is then tackled based on different performance metrics, e.g., sum rate [11], [12], coverage probability [13], [14], and (coded or uncoded) bit error rate (BER) [15]. Assuming perfect statistics of the channel state information (CSI), an expression of the downlink achievable rate for matched-filter precoding has been derived in [16]. Moreover, the performance of quantized transceivers in MU-MIMO downlink has been investigated in [17], [18]. Robust 1-bit massive MU-MIMO precoding designs for very large scale integration (VLSI) systems have been studied in [19], which narrowed the gap between theoretical study and technological application. More importantly, it has been shown in a recent study [20] that, compared with massive MIMO systems using ideal DACs, the performance (sum rate) loss in 1-bit DACs based massive MU-MIMO systems can be compensated by disposing approximately 2.5 times more antennas at the BS.

In brief summary, for an MU-MIMO downlink system with 1-bit DACs, linear quantized precoders could greatly reduce the power consumption and significantly simplify the industrial design of the device in the BS. However, linear quantized precoders have to pay a high price for system performance in terms of BER, especially when the communication systems are applied with the high-order QAM modulation technique.

Alternatively, the nonlinear analysis has the capability to significantly outperform linear analysis at the cost of additional computational complexity. For example, in a recent work [21], a new precoding method has been proposed to mitigate

Lily Li and Dr. Qiu is with the Department of Electrical and Computer Engineering Tennessee Technological University, Cookeville, TN 38505 USA. Dr. Qiu is also with Department of Electrical Engineering, Research Center for Big Data and Artificial Intelligence Engineering and Technologies, Shanghai Jiaotong University, Shanghai 200240, China. (e-mail: rqiu@ieee.org).

Lei Chu is with Department of Electrical Engineering, Research Center for Big Data Engineering Technology, Shanghai Jiaotong University, Shanghai 200240, China. (leochu@sjtu.edu.cn)

Fei Wen is with the Department of Electronic Engineering, Shanghai Jiao Tong University, Shanghai 200240, China.

Dr. Qiu's work is partially supported by N.S.F. of China under Grant No.61571296 and N.S.F. of US under Grant No. CNS-1619250.

the inter-user-interference and channel distortion in a 1-bit downlink MU-MISO system with QPSK symbols. Meanwhile, for 1-bit MU-MIMO, semidefinite relaxation (SDR) based precoding has been brought up in [22], where the SDR precoder is about 3dB worse compared with the ideal case for an uncoded BER of 10^{-3} . However, the high computational complexity of the SDR method is the major obstacle to its application in massive MU-MIMO with a large number of antennas. To address this limitation, an efficient squared-infinity norm Douglas-Rachford splitting (SQUID) based precoder has been proposed more recently in [23], [24]. Compared with the SDR method, the SQUID method is much more efficient, but has worse performance due to the removal of the nonconvex constraint in the original precoding problem.

The goal of this work is to develop a highly efficient and effective algorithm for the nonlinear precoding problem in 1-bit MU-MIMO. The main contributions are as follows.

B. Contributions

First, we propose an efficient algorithm to solve the nonlinear precoding problem based on the alternative direction method of multipliers (ADMM) framework. The nonlinear precoding problem is generally difficult to solve due to the nonconvex constraint, which enforces the elements of the solution vector to have a uniform modulus. Unlike the SDR and SQUID algorithms solving convex relaxed versions of the original nonconvex precoding problem, we solve the nonconvex precoding problem directly via first reformulating it into an unconstrained form. The SQUID algorithm is also based on the ADMM framework, but it involves double loops in the iteration procedure, as an inner loop is needed to solve the proximal operator for the squared ℓ_∞ -norm. In comparison, our algorithm has a single loop and thus is more efficient. Meanwhile, since the new algorithm does not relax the original problem, it can be expected to achieve better performance than the SQUID algorithm.

Second, a sufficient condition for the convergence of the new algorithm has been derived. Since the nonlinear precoding problem is nonconvex and nonsmooth, the convergence condition of the new algorithm is important for its stable implementation in applications. The results indicate that, the new algorithm is globally convergent under a rather weak condition, e.g., provided that the penalty parameter is selected sufficiently large.

Finally, we have compared the new algorithm with some state-of-the-art algorithms via numerical simulations in various conditions. The results demonstrated that, the new algorithm can achieve state-of-the-art performance, while being of the most efficient among the nonlinear quantized precoders, e.g., more than 300 times faster than the SDR algorithm in terms of run time.

C. Paper Outline and Notations

The remainder of this paper is structured as follows. Section II introduces the mathematical assumptions and outlines the system models. For a better understanding on the motivation of the development of the proposed algorithm, a brief review on

the recently advanced linear and nonlinear quantized precoders is given in Section III. We then present the proposed nonlinear quantized precoder in Section IV. In Section V, numerical studies are provided to evaluate the efficiency and effectiveness of the proposed nonlinear precoding algorithm. The conclusion of this paper is given in Section VI. For the sake of simplicity, auxiliary technical derivations are deferred to the Appendix.

Notations: Throughout this paper, vectors and matrices are given in lower and uppercase boldface letters, e.g., \mathbf{x} and \mathbf{X} , respectively. $[\mathbf{X}]_{kl}$ denotes the element at the k th row and l th column. The symbols $\text{diag}(\mathbf{X})$, $\text{tr}(\mathbf{X})$, $\mathbb{E}[\mathbf{X}]$, \mathbf{X}^* , and \mathbf{X}^T denote the diagonal operator, trace operator, expectation operator, the conjugate, and the transpose of \mathbf{X} , respectively. We use $\Re(\mathbf{x})$, $\Im(\mathbf{x})$, and $\|\mathbf{x}\|_2$ to represent the real part, the imaginary part, ℓ_2 -norm of vector \mathbf{x} . $\mathbf{A} \succeq \mathbf{0}$ means \mathbf{A} is nonnegative definite. $\partial f(\cdot)$ stands for the subdifferential of the function f . $\text{sign}(\cdot)$ denotes the sign of a quantity with $\text{sign}(0) = 0$. \mathbf{I} is an identity matrix with proper size. $\text{dist}(\mathbf{x}, S) := \inf\{\|\mathbf{y} - \mathbf{x}\|_2 : \mathbf{y} \in S\}$ denotes the distance from a point $\mathbf{x} \in \mathbb{R}^n$ to a subset $S \in \mathbb{R}^n$. $\text{eig}_{\min}(\cdot)$ and $\text{eig}_{\max}(\cdot)$ denote the minimal and maximal eigenvalues of a matrix, respectively. \oslash denotes the element-wise division operation. $\mathbf{1}$ is a column vector with all elements be 1.

II. SYSTEM MODEL

A. Mathematical Assumptions and Notations

In this work, we conduct analysis under assumption of perfect synchronization of the transmit antennas and perfect recovery of frame synchronization at the UTs [4], [10], [16], [19], [25]. The channel remains unchanged in one coherence time. Besides, it is assumed that the BS has the perfect knowledge of CSI. We will relax such an assumption and investigate the sensitivity of the proposed nonlinear precoding algorithm in the case of imperfect CSI in Section V.

Besides, to efficiently acquire CSI at each user in the massive MU-MIMO downlink [26], [27], we prefer a open-loop training under time-division duplex (TDD) operation to frequency-division duplex (FDD) operation¹.

B. MU-MIMO Downlink System with One-bit DACs

As shown in Fig. 1, we consider a single-cell quantized massive MU-MIMO downlink system with U single-antenna UTs and a R -antenna base station (BS), in which each antenna is equipped with two 1-bit DACs. Let $\mathbf{s} \in \mathbb{C}^{U \times 1}$ be the constellation points to be sent to UTs. Using the knowledge of CSI, the BS precodes the \mathbf{s} into a R -dimensional vector $\mathbf{x} = \mathbf{P}\mathbf{s}$, where $\mathbf{P} \in \mathbb{C}^{R \times U}$ is the precoding matrix. The precoded symbols \mathbf{x} satisfies the average power constraint [4], [29]

$$\mathbb{E}_{\mathbf{s}} [\mathbf{x}\mathbf{x}^T] \leq P_{TX}. \quad (1)$$

¹The number of downlink resources needed for pilots is proportionate to the number of BS antennas in FDD and the number of users in TDD [28], respectively. And the number of BS antennas is typically much bigger than the number of UT in a massive MU-MIMO system.

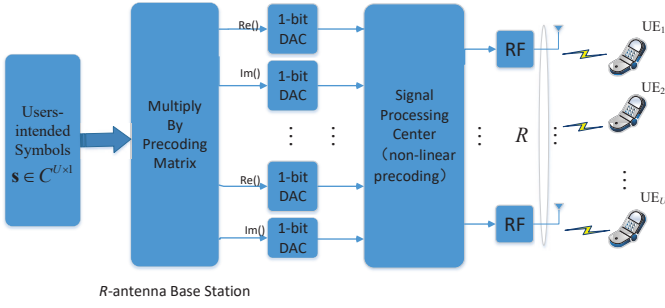


Fig. 1. The framework of the massive MU-MIMO downlink system with 1-bit DACs.

The BS tries to send data symbols $\mathbf{x} \in \mathbb{C}^{R \times 1}$ simultaneously to UTs over $U \times R$ memoryless Gaussian block-fading channel \mathbf{H} . For the MU-MIMO downlink systems with infinite-resolution DACs, the received signal at UTs is

$$\mathbf{y} = \sqrt{\rho} \mathbf{H} \mathbf{x} + \mathbf{n}, \quad (2)$$

where \mathbf{n} is a complex vector with element n_i being complex additive Gaussian noise distributed as $n_r \sim \mathcal{CN}(0, \varepsilon^2)$ and ρ is the channel gain. The signal-to-noise (SNR) is defined by $\alpha = P/\varepsilon^2$. In the following analysis, we will employ the channel model introduced in [16], which is given by

$$\mathbf{H} = \text{diag}(\sigma_1^2, \dots, \sigma_U^2) \bar{\mathbf{H}}, \quad (3)$$

where the entries of $\bar{\mathbf{H}}$ are complex Gaussian random variables, whose real and imaginary parts are assumed to be independent and identically distributed zero-mean Gaussian random variables with unit variance; σ_u^2 denotes potential path loss for u -th user.

For the case of the massive MU-MIMO with 1-bit DACs, each precoded signal component x_i , $i = 1, \dots, R$ is quantized separately into a finite set of prescribed labels by a 1-bit uniform quantizer Q . It is assumed that the real and imaginary parts of precoded signals are quantized separately. The resulting quantized signals read

$$\begin{aligned} \mathbf{z} &= Q(\mathbf{P}\mathbf{s}) = Q(\mathbf{x}) \\ &= Q(\Re(\mathbf{x})) + jQ(\Im(\mathbf{x})) \\ &= \kappa(\text{sign}(\Re(\mathbf{x})) + j \text{sign}(\Im(\mathbf{x}))) \end{aligned} \quad (4)$$

where κ is set to $\kappa = \sqrt{P_{TX}/2R}$ in order to satisfy the power constraint in (1). In what follows, the output set of the 1-bit quantization is defined as $\Omega_1 = \kappa\{1+j, 1-j, -1+j, -1-j\}$.

Finally, the input-output relationship of the MU-MIMO downlink system with 1-bit DACs can be denoted as

$$\mathbf{y} = \sqrt{\rho} \mathbf{H} Q(\mathbf{x}) + \mathbf{n} = \sqrt{\rho} \mathbf{H} \mathbf{z} + \mathbf{n}. \quad (5)$$

The precoding problem based on ideal model in (2) has been investigated extensively by checking different performance metrics, i.e. throughput and mean square error (MSE) between received signal and transmitted signal. However, for the case of the quantized massive MU-MIMO (5), the precoding problem should be revisited carefully as the precoded symbols at BS are affected by extra distortion introduced by low-resolution DACs. The detailed analysis is shown in the following.

III. QUANTIZED PRECODING PROBLEMS AND SOLUTIONS

A. Linear Quantized Problem and Solutions

We start by briefly investigating the recently advanced linear quantized precoders, in which their advantages are explored and related limitations are also discussed.

For the precoding problem of the quantized MU-MIMO systems as introduced in (5), one can formulate the precoding problem by minimizing the MSE between the intended signal \mathbf{s} and the quantized precoded signal $Q(\mathbf{P}\mathbf{s})$ through the channel \mathbf{H} as follows:

$$\begin{aligned} &\text{minimize}_{\mathbf{P}, \rho} \quad \|\mathbf{s} - \rho \mathbf{H} Q(\mathbf{P}\mathbf{s})\|_2^2 + \rho^2 U \varepsilon^2 \\ &\text{subject to} \quad \|Q(\mathbf{P}\mathbf{s})\|_2^2 \leq P_{TX}, \rho > 0 \end{aligned} \quad (6)$$

It is difficult to tackle the problem in (6) directly as the nonlinear operation of the employed 1-bit DACs. On the other hand, using the well-known Bussgang theorem [7], one can decompose the nonlinear quantized signal output into a linear function of the input to the quantizers and an uncorrelated distortion term. Specially, we have

$$\mathbf{z} = Q(\mathbf{P}\mathbf{s}) = \mathbf{G}\mathbf{P}\mathbf{s} + \mathbf{w}. \quad (7)$$

For the case of 1-bit DACs, it is a common assumption in the previous studies that the unknown \mathbf{G} is considered to be a diagonal matrix in the low-SNR regime [5], [10], [14], [16], [19], [20], [22]. Besides, by means of mathematical derivation, the diagonal elements can be approximately calculated as follows:

$$[\mathbf{G}]_{11} = \dots = [\mathbf{G}]_{RR} = \sqrt{2/\pi}. \quad (8)$$

Substituting (7) and (8) in to (6), one can solve the precoding problem with similar technologies (i.e., MRT, ZF or WF), which are widely used in MU-MIMO communications systems with infinite-resolution DACs [4].

The linear quantized precoders could greatly reduce the power consumption and significantly simplify the industrial design of the device in the BS. However, linear quantized precoders have to pay high price for the system performance in terms of BER, especially when the communication systems are applied with the high-order QAM modulation techniques. With an aim to achieve the goal of closing the performance gap², we will briefly investigate the nonlinear precoding methods in Section III-B and provide an efficient and robust nonlinear quantized precoder in Section IV.

B. Nonlinear Quantized Problem and Solutions

1) *Nonlinear Quantized Precoding Problem:* Alternatively, nonlinear precoding algorithms could achieve higher performance gain in term of bit error rate. In the 1-bit case, the outputs of DACs share same amplitude: $\|\mathbf{z}\|_2^2 = \|Q(\mathbf{P}\mathbf{s})\|_2^2 = P_{TX}$. By minimizing the MSE of intended symbols \mathbf{s} and quantized outputs \mathbf{z} , the 1-bit nonlinear precoding problem can be formulated as

²It is proven in recent study [20] that, compared with massive MIMO systems with ideal DACs, the sum rate loss in 1-bit massive MU-MIMO systems can be compensated for by disposing approximately 2.5 times more antennas at the BS. Accordingly, we will restrict us by developing possible precoding algorithms in regard to reducing bit error rate.

$$\begin{aligned} & \underset{\mathbf{z} \in \Omega_1}{\text{minimize}} && \|\mathbf{s} - \rho \mathbf{H} \mathbf{z}\|_2^2 + \rho^2 U \varepsilon^2 \\ & \text{subject to} && \|\mathbf{z}\|_2^2 = P_{TX}, \rho > 0 \end{aligned} \quad (9)$$

Regardless of the effect of the noise, one might seek to develop a maximum likelihood based nonlinear quantized precoder [30] which attempts to solve

$$\underset{\mathbf{z} \in \Omega_1}{\text{minimize}} \quad \|\mathbf{s} - \rho \mathbf{H} \mathbf{z}\|_2^2. \quad (10)$$

The problem in (10) can be tackled by the naive exhaustive search (NES) [31] with complexity of order $O(4^R)$ or by sphere decoding (SD) [32] with exponential complexity. The prohibitive computational complexities of these methods impede their application in small-size or middle-size MIMO cases, let alone in massive MU-MIMO systems.

On the other hand, an efficient approach for the nonlinear precoding problem is based on SDR, which is a well-known technique that has been widely used for tackling discrete variables optimization problem, i.e., MIMO Detection for high-order QAM constellations [33] and binary quadratic minimization [34]. We highlight the SDR precoder as the benchmark algorithm as it has been shown in [34] that SDR can provide a provably near-optimal solution, achieving a constant factor approximation of the optimal solution in probability. The SDR based precoding method has the advantage of sound theoretical guarantees and work well in practice. The disadvantage is that, with complexity of $O((2R+1)^{4.5})$ at the worst-case [35], [36], the SDR precoder cannot handle high-dimensional problem sizes, e.g., the massive MU-MIMO systems with hundreds of antennas, which motivates us to develop a more efficient solution.

IV. THE PROPOSED PRECODING ALGORITHM

Unlike traditional methods solving relaxed formulations of (9) as it is nonconvex, e.g., SDR [27] and ℓ_∞ relaxation [22], in this section we present an efficient ADMM algorithm to directly solve the problem (9) by first reformulating it into an unconstrained form. Although the reformulated problem is nonconvex and nonsmooth, we derive a sufficient condition under which the proposed ADMM algorithm is globally convergent.

A. Algorithm

ADMM is a powerful framework well suited to solve many high-dimensional optimization problems and has been widely applied in signal/image processing [37]–[39], statistics [40] and machine learning [41]. ADMM utilizes a decomposition-coordination procedure to naturally decouple the variables in the global problem, which makes the global problem easy to tackle.

First, denote $\mathbf{v} = \rho \mathbf{z}$ and

$$\begin{aligned} \tilde{\mathbf{s}} &= \begin{bmatrix} \Re(\mathbf{s}) \\ \Im(\mathbf{s}) \end{bmatrix}, & \tilde{\mathbf{v}} &= \begin{bmatrix} \Re(\mathbf{v}) \\ \Im(\mathbf{v}) \end{bmatrix}, \\ \tilde{\mathbf{H}} &= \begin{bmatrix} \Re(\mathbf{H}) & -\Im(\mathbf{H}) \\ \Im(\mathbf{H}) & \Re(\mathbf{H}) \end{bmatrix}. \end{aligned} \quad (11)$$

Then, using the fact that $\mathbb{E} \left\{ \|\mathbf{z}\|_2^2 \right\} = P_{TX}$, the complex-valued problems in (9) can be equivalently expressed as a real-valued problem as

$$\begin{aligned} & \underset{\tilde{\mathbf{v}}}{\text{minimize}} && \left\| \tilde{\mathbf{s}} - \tilde{\mathbf{H}} \tilde{\mathbf{v}} \right\|_2^2 + \frac{U \varepsilon^2}{P_{TX}} \|\tilde{\mathbf{v}}\|_2^2 \\ & \text{subject to} && \tilde{\mathbf{v}} \in \Omega \end{aligned} \quad (12)$$

where $\Omega = \{\pm \kappa \rho, \rho > 0\}$. Denote the constraint $\tilde{\mathbf{v}} \in \Omega$ as $[\tilde{\mathbf{v}}]_1^2 = \dots = [\tilde{\mathbf{v}}]_{2R}^2$, the nonlinear quantized precoding problem in (12) can be reformulated as [36], [22]

$$\begin{aligned} & \underset{\tilde{\mathbf{v}}}{\text{minimize}} && \left\| \tilde{\mathbf{s}} - \tilde{\mathbf{H}} \tilde{\mathbf{v}} \right\|_2^2 + \frac{U \varepsilon^2}{P_{TX}} \|\tilde{\mathbf{v}}\|_2^2 \\ & \text{subject to} && [\tilde{\mathbf{v}}]_1^2 = \dots = [\tilde{\mathbf{v}}]_{2R}^2 \end{aligned} \quad (13)$$

Let $\delta_\Omega(\mathbf{o})$ denote the indicator function defined on the set Ω as

$$\delta_\Omega(\mathbf{o}) = \begin{cases} 0, & \mathbf{o} \in \Omega \\ \infty, & \text{otherwise} \end{cases}. \quad (14)$$

Then, the problem (13) can be rewritten as

$$\underset{\tilde{\mathbf{v}}}{\text{minimize}} \quad f(\tilde{\mathbf{v}}) \quad (15)$$

where

$$f(\tilde{\mathbf{v}}) = \left\| \tilde{\mathbf{s}} - \tilde{\mathbf{H}} \tilde{\mathbf{v}} \right\|_2^2 + c \|\tilde{\mathbf{v}}\|_2^2 + \delta_\Omega(\tilde{\mathbf{v}})$$

with $c = U \varepsilon^2 / P_{TX}$. With this new formulation (15), we can solve the problem (9) using the efficient ADMM framework, which decouples the unknown variables and tackles the problem in an efficient manner. Specially, the problem (15) can be equivalently expressed as

$$\begin{aligned} & \underset{\tilde{\mathbf{v}}}{\text{minimize}} && \left\| \tilde{\mathbf{s}} - \tilde{\mathbf{H}} \tilde{\mathbf{v}} \right\|_2^2 + c \|\tilde{\mathbf{v}}\|_2^2 + \delta_\Omega(\mathbf{u}) \\ & \text{subject to} && \tilde{\mathbf{v}} - \mathbf{u} = \mathbf{0} \end{aligned} \quad (16)$$

where \mathbf{u} is an auxiliary variable. The augmented Lagrangian associated with the problem (16) is

$$\begin{aligned} \mathcal{L}_\lambda(\tilde{\mathbf{v}}, \mathbf{u}, \mathbf{w}) &= g(\tilde{\mathbf{v}}, \mathbf{u}) - \langle \mathbf{w}, \tilde{\mathbf{v}} - \mathbf{u} \rangle + \frac{\lambda}{2} \|\tilde{\mathbf{v}} - \mathbf{u}\|_2^2 \\ &= g(\tilde{\mathbf{v}}, \mathbf{u}) + \frac{\lambda}{2} \left\| \tilde{\mathbf{v}} - \mathbf{u} - \frac{\mathbf{w}}{\lambda} \right\|_2^2 - \frac{\|\mathbf{w}\|_2^2}{2\lambda} \end{aligned} \quad (17)$$

where

$$g(\tilde{\mathbf{v}}, \mathbf{u}) = \left\| \tilde{\mathbf{s}} - \tilde{\mathbf{H}} \tilde{\mathbf{v}} \right\|_2^2 + c \|\tilde{\mathbf{v}}\|_2^2 + \delta_\Omega(\mathbf{u})$$

and \mathbf{w} is the dual variable, $\lambda > 0$ accounts for the penalty factor related to the argumentation. Then, ADMM applied to the problem (17) consists of the following three steps in the $(k+1)$ -th iteration

$$\mathbf{u}^{k+1} = \arg \min_{\mathbf{u}} \left(\delta_\Omega(\mathbf{u}) + \frac{\lambda}{2} \left\| \tilde{\mathbf{v}}^k - \mathbf{u} - \frac{\mathbf{w}^k}{\lambda} \right\|_2^2 \right) \quad (18)$$

$$\begin{aligned} \tilde{\mathbf{v}}^{k+1} &= \arg \min_{\tilde{\mathbf{v}}} \left(\left\| \tilde{\mathbf{s}} - \tilde{\mathbf{H}} \tilde{\mathbf{v}} \right\|_2^2 + c \|\tilde{\mathbf{v}}\|_2^2 \right. \\ &\quad \left. + \frac{\lambda}{2} \left\| \tilde{\mathbf{v}} - \mathbf{u}^{k+1} - \frac{\mathbf{w}^k}{\lambda} \right\|_2^2 \right) \end{aligned} \quad (19)$$

$$\mathbf{w}^{k+1} = \mathbf{w}^k - \lambda (\tilde{\mathbf{v}}^{k+1} - \mathbf{u}^{k+1}). \quad (20)$$

The $\tilde{\mathbf{v}}$ -subproblem (19) is quadratic which has a closed-form solution given by

$$\tilde{\mathbf{v}}^{k+1} = [2\mathbf{H}^T\mathbf{H} + (2c + \lambda)\mathbf{I}]^{-1} (2\mathbf{H}^T\tilde{\mathbf{s}} + \lambda\mathbf{u}^{k+1} + \mathbf{w}^k). \quad (21)$$

The \mathbf{u} -subproblem (18) is a projection of $(\mathbf{v}^k - \mathbf{w}^k/\lambda)$ onto the set Ω , whose solution is given by

$$\mathbf{u}^{k+1} = \text{sign}(\mathbf{v}^k - \mathbf{w}^k/\lambda) \frac{\|\mathbf{v}^k - \mathbf{w}^k/\lambda\|}{2R}. \quad (22)$$

Finally, let $\hat{\mathbf{v}}$ denote the solution of the above ADMM algorithm, using the rounding strategy as described in [36], we can obtain the desired real-valued precoded vector by

$$\hat{\mathbf{z}} = \kappa \text{sign}[\hat{\mathbf{v}}]. \quad (23)$$

Then, the complex-valued precoded vector can be determined as

$$\tilde{\mathbf{z}} = [\hat{\mathbf{z}}]_{1:R} + j[\hat{\mathbf{z}}]_{R+1:2R}. \quad (24)$$

In this ADMM algorithm, if the penalty parameter λ does not change in the iteration procedure, we only need to compute the matrix inversion in the $\tilde{\mathbf{v}}$ -update (21) once. Besides, the dominant computational load in each iteration is matrix-vector multiplication with complexity $O(R^2)$.

B. Convergence Analysis

As the set Ω is nonconvex, the problem (15) is nonconvex and nonsmooth. While the convergence properties of ADMM have been well established for the convex case, there have been only a few studies reported very recently for the nonconvex case. For the convex case, the convergence of the ADMM algorithm is easily guaranteed. But for the nonconvex case, the convergence of the ADMM algorithm relies on the property of the objective function and the selection of the penalty parameter. In the following, we derive a sufficient condition for the convergence of the proposed ADMM algorithm using the approach in [40].

We first give three lemmas for deriving the sufficient condition. The proofs are given in Appendix. In the sequel for convenience we use the notations: $\varphi_1 = \text{eig}_{\min}(\mathbf{H}^T\mathbf{H})$ and $\varphi_2 = \text{eig}_{\max}(\mathbf{H}^T\mathbf{H})$, which denote the minimal and maximal eigenvalues of $\mathbf{H}^T\mathbf{H}$, respectively.

Lemma I. The sequence $\{(\tilde{\mathbf{v}}^k, \mathbf{u}^k, \mathbf{w}^k)\}$ generated via (18)–(20) satisfies

$$\begin{aligned} \mathcal{L}(\tilde{\mathbf{v}}^{k+1}, \mathbf{u}^{k+1}, \mathbf{w}^{k+1}) &\leq \mathcal{L}(\tilde{\mathbf{v}}^k, \mathbf{u}^k, \mathbf{w}^k) \\ &\quad - \left[\frac{2\varphi_1 + 2c + \lambda}{2} - \frac{4(\varphi_2 + c)^2}{\lambda} \right] \|\tilde{\mathbf{v}}^{k+1} - \tilde{\mathbf{v}}^k\|_2^2. \end{aligned}$$

In particular, if (25) holds, \mathcal{L} is monotonously decreasing in the iteration procedure.

Lemma I implies that, under the condition (25), \mathcal{L} is nonincreasing in the iteration and thus is convergent as it is lower semi-continuous.

Lemma II. For the sequence $\{(\tilde{\mathbf{v}}^k, \mathbf{u}^k, \mathbf{w}^k)\}$ generated via (18)–(20), denote $\mathbf{z}^k := (\tilde{\mathbf{v}}^k, \mathbf{u}^k, \mathbf{w}^k)$, suppose that (25) holds, then

$$\lim_{k \rightarrow \infty} \|\mathbf{z}^{k+1} - \mathbf{z}^k\|_2^2 = 0.$$

In particular, any cluster point of $\{(\tilde{\mathbf{v}}^k, \mathbf{u}^k, \mathbf{w}^k)\}$ is a stationary point of \mathcal{L} .

Lemma III. For the sequence $\{(\tilde{\mathbf{v}}^k, \mathbf{u}^k, \mathbf{w}^k)\}$ generated via (18)–(20), suppose that (25) holds, then there exists a constant $c_0 > 0$ such that

$$\text{dist}(0, \partial\mathcal{L}(\tilde{\mathbf{v}}^k, \mathbf{u}^k, \mathbf{w}^k)) \leq c_0 \|\tilde{\mathbf{v}}^{k+1} - \tilde{\mathbf{v}}^k\|_2^2.$$

Lemma III establishes a subgradient lower bound for the iterate gap, which together with Lemma II implies that $\text{dist}(0, \partial\mathcal{L}(\tilde{\mathbf{v}}^k, \mathbf{u}^k, \mathbf{w}^k)) \rightarrow 0$ as $k \rightarrow \infty$.

Based on the results in the above lemmas, we can conclude the following theorem.

Theorem I. Suppose that the penalty parameter λ satisfies

$$\lambda > \max \left(\sqrt{(\varphi_1 + c)^2 + 8(\varphi_2 + c)^2} - \varphi_1 - c, 8\varphi_2, 8c \right) \quad (25)$$

then, the sequence $\{(\tilde{\mathbf{v}}^k, \mathbf{u}^k, \mathbf{w}^k)\}$ generated by the ADMM steps (18)–(20) converges to a stationary point of the problem (15).

C. Efficient Implementation of the Proposed Algorithm

This result in Theorem I implies that, the proposed ADMM algorithm is globally convergent if the penalty parameter λ is selected sufficiently large to satisfy (25). To further accelerate the ADMM algorithm, a standard trick is to using a continuation process for the penalty parameter λ . More specifically, use a properly small starting value of it and gradually increase it by iteration until reaching the target value satisfying the condition (25), e.g., $\lambda_0 \leq \dots \leq \lambda_K = \lambda_{K+1} = \dots = \lambda$. Theorem I still applies if the value of λ becomes fixed after a finite number of iterations.

Besides, it is noted that the dynamic adjusting of λ will result in performing matrix inversion in (21) in each iteration. In fact, we only need to compute matrix inverse only once in the first iteration by using the fact that $\mathbf{H}^T\mathbf{H}$ is a symmetric matrix. Specifically, in the first iteration, we can perform the singular value decomposition (SVD) of $\mathbf{H}^T\mathbf{H}$ to yield $(\mathbf{U}, \mathbf{S}, \mathbf{U}^T) = \text{svd}(\mathbf{H}^T\mathbf{H})$; \mathbf{U} contains the singular vectors and $\mathbf{U}\mathbf{U}^T = \mathbf{I}$. Then, denote $(\mathbf{S} + \alpha\mathbf{I})^{-1} = \text{diag}(\mathbf{a})$, using the matrix inversion formulas

$$(\mathbf{ABC})^{-1} = \mathbf{C}^{-1}\mathbf{B}^{-1}\mathbf{A}^{-1}$$

$$(\mathbf{USU}^T + \alpha\mathbf{I})^{-1} = \mathbf{U}(\mathbf{S} + \alpha\mathbf{I})^{-1}\mathbf{U}^T$$

and the relation

$$\text{diag}(\mathbf{a})^{-1}\mathbf{U}^T\mathbf{c} = \mathbf{U}^T\mathbf{c} \oslash \mathbf{a},$$

we can efficiently update the $\tilde{\mathbf{v}}$ -subproblem in the subsequent iterations as

$$\begin{aligned} \tilde{\mathbf{v}}^{k+1} &= [2\mathbf{H}^T\mathbf{H} + (2c + \lambda^{k+1})\mathbf{I}]^{-1} \\ &\quad \times (2\mathbf{H}^T\tilde{\mathbf{s}} + \lambda^{k+1}\mathbf{u}^{k+1} + \mathbf{w}^k) \quad (26) \\ &= \mathbf{U} [(\mathbf{U}^T(2\mathbf{H}^T\tilde{\mathbf{s}} + \lambda^{k+1}\mathbf{u}^{k+1} + \mathbf{w}^k)) \oslash \hat{\mathbf{s}}] \end{aligned}$$

where

$$\hat{\mathbf{s}} = 2\text{diag}(\mathbf{S}) + (2c + \lambda^{k+1})\mathbf{1}.$$

In this manner, the dominant computation load in each subsequent iteration is matrix-vector multiplication with computational complexity $O(R^2)$, which improves the efficiency of the proposed algorithm.

V. SIMULATIONS

This section evaluates the performance of the new algorithm via numerical simulations in comparison with two state-of-the-art nonlinear quantized precoders, SDR [12] and SQUID [19], [23], and three linear quantized precoders, MRT, WF and ZF [4], [16]. The proposed algorithm is initialized with zero, and the penalty parameter λ is selected to satisfy the convergence condition (25). Each provided result is an average over 1000 independent runs (except for the results in Fig. 2, where only one simulation for each condition to illustrate the convergence behavior).

A. Convergence Behavior of the Proposed Precoder

First, we show the convergence behavior of the proposed algorithm by investigating the iterate gap of the $\tilde{\mathbf{v}}$ and \mathbf{u} variables, defined as

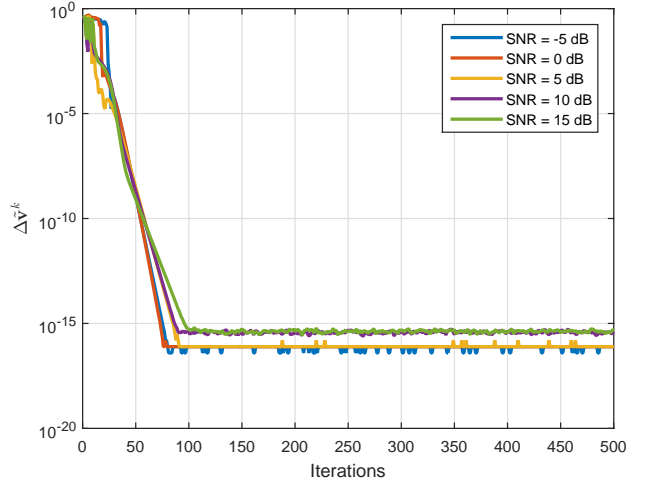
$$\begin{aligned} \Delta \tilde{\mathbf{v}}^k &= \|\tilde{\mathbf{v}}^{k+1} - \tilde{\mathbf{v}}^k\|_2 \\ \Delta \mathbf{u}^k &= \|\mathbf{u}^{k+1} - \mathbf{u}^k\|_2. \end{aligned} \quad (27)$$

We consider a MU-MIMO system with 16 BS antennas and 4 UTs, with a wide range of the SNR values. Fig. 2 shows the typical convergence behavior of the proposed precoder. The results in Fig. 2 demonstrate that the proposed algorithm is convergent and it can converge to a sufficient accuracy within only tens of iterations. For example, it can converge to an accuracy with tolerance lower than 10^{-7} within only 50 iterations in a wide range of SNR values.

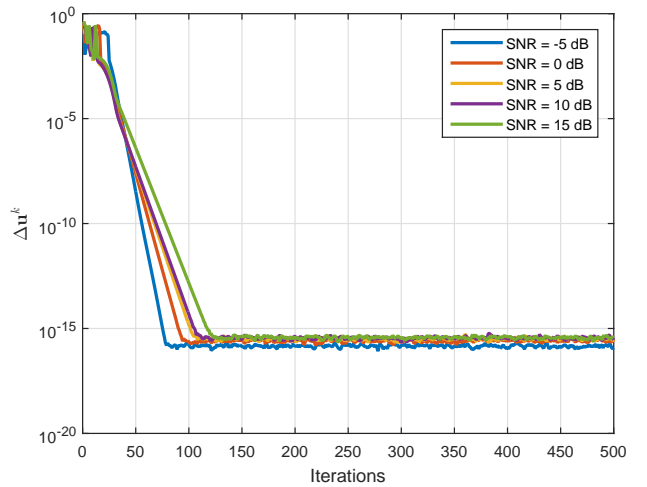
B. Computational Complexity Comparison

We consider a MU-MIMO system with R -antenna and 4 UTs. The numbers of antennas are 16, 32, 64, 128 and 256, respectively. The SDR based precoder has a computational complexity of $O((2R+1)^{4.5})$ at the worst-case, the SQUID precoder with two loops has a computational complexity of $O(2(k_1R^3 + k_2R^2))$ (k_1 and k_2 are the iteration numbers of the two loops), while the proposed precoder only requires SVD of complexity $O(R^3)$ once in the first iteration and the dominant computation load in each of the subsequent iterations is matrix-vector multiplication of complexity $O(R^2)$ in each of the subsequent iterations.

Fig. 3 compares the run time of the algorithms versus different number of antennas. The algorithms are performed on a desktop PC with an Intel Core I7-7700K CPU at 4.2 GHz with 32 GB RAM. It can be seen that, the proposed precoder outperforms the compared nonlinear quantized precoders for any number of the antennas. For example, the run time of the SQUID and SDR precoders are respectively about 3 times and remarkably about 380 times that of the new precoder. The linear quantized precoders, MRT, ZF and WF, have significantly lower complexity than the nonlinear quantized precoders. However, as will be shown in the later



(a) Iterate gap of the $\tilde{\mathbf{v}}$ variable



(b) Iterate gap of the \mathbf{u} variable

Fig. 2. Typical convergence behavior of the proposed algorithm in different SNR.

experiments, the performance of the linear quantized precoders are significantly worse than that of the nonlinear quantized precoders.

C. Uncoded BER Performance

We compare the performance of the new precoder and other involved precoders in the view of uncoded BER with QPSK signaling. The ZF precoder with infinite-resolution DACs (ZFi) is regarded as the benchmark.

Fig. 4 shows the performance of the precoders in the case of a small size MU-MIMO system equipped with 16 BS antennas and serving 4 UTs. It can be seen that, the performance of the nonlinear quantized precoders, SQUID, SDR, and the proposed precoder, surpasses that of the linear quantized precoders, MRT, ZF and WF, in most cases. The benefit of using a nonlinear quantized precoder is especially conspicuous for moderate to relatively high SNR, as the advantage of

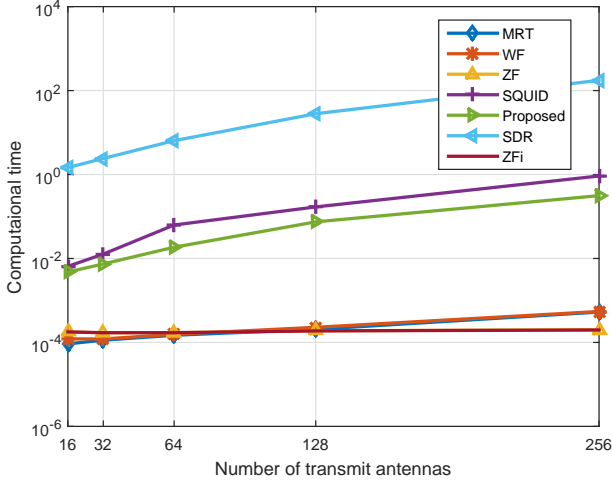


Fig. 3. Runtime comparison of the compared precoders versus the number of the BS antennas.

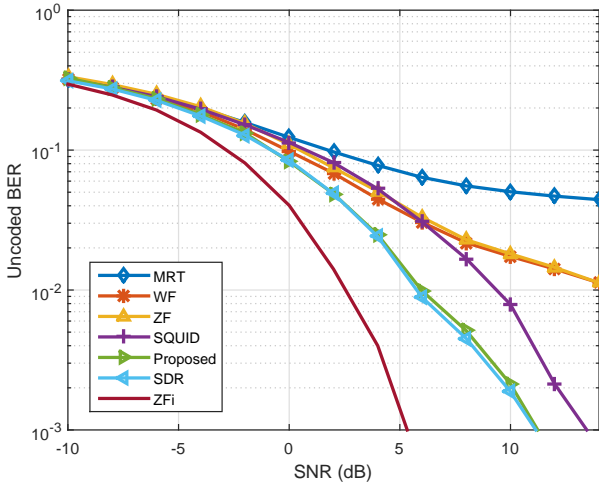


Fig. 4. Uncoded BER of the compared precoders in the case of a small size MU-MIMO system (16 BS antennas and 4 UTs) with QPSK signaling.

the nonlinear quantized precoders over the linear quantized precoders increase as the SNR increases.

Fig. 5 represents the result in the case of a massive MU-MIMO with 128 BS antennas and 20 UTs. It can be seen from Fig. 5 that, the linear quantized precoders tend to be saturated as the SNR increases. Specially, the BERs do not decrease distinctly as the SNR increases when the SNR is above a certain threshold. In comparison, the nonlinear quantized precoders have significantly better performance in moderate to relatively high SNR.

From Fig. 4 and Fig. 5, the performance of each precoder improves as the number of the BS antennas increases. The SDR precoder and the proposed precoder generally perform comparably in most cases. In the case of a small size MU-MIMO system with 16 antennas, the SDR precoder and the proposed precoder significantly outperform the SQUID precoder, e.g., when $\text{SNR} > 0$ dB. But in the case of a large

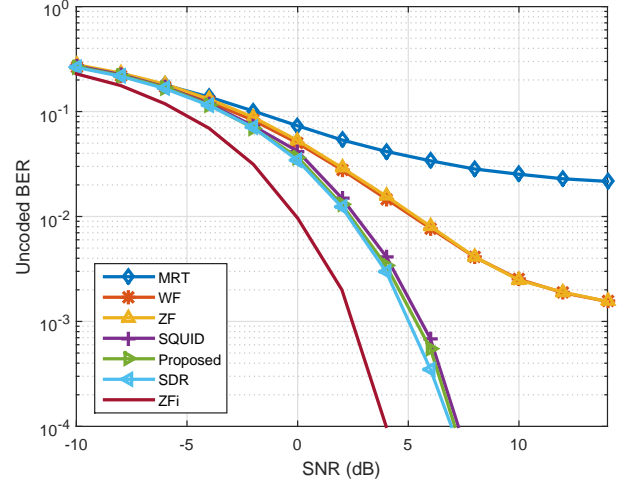


Fig. 5. Uncoded BER of the compared precoders in the case of a large size MU-MIMO system (128 BS antennas and 20 UTs) with QPSK signaling.

size MU-MIMO system with 128 antennas, the advantage of the SDR precoder and the proposed precoder over the SQUID precoder is no longer so prominent and becomes marginal. In short, the results in Fig. 4 and Fig. 5 implies that the disparities between the ideal MU-MIMO system and the system with 1-bit DACs can be reduced by increasing the number of the BS antennas and by employing proper signal processing techniques.

D. Effect of Different Modulation Modes

This experiment investigates the proposed precoder for different modulation schemes, QPSK, 16QAM and 64QAM. We consider a MU-MIMO system with 128 BS antennas and 10 UTs. Fig. 6 presents the performance of the proposed precoder compared with the ideal ZFi precoder (with infinite-resolution DACs as benchmark) in the three modulation modes. The results in Fig. 6 indicate that the proposed precoder can provide reliable transmission of QPSK signaling and well support the high modulation mode 16QAM. But for the case of 64QAM, reliable transmission is in need of more antennas and/or more sophisticated techniques that we leave them in our forthcoming work.

E. Effect of the Channel Estimation Error

We now investigate the effect of the channel estimation error. Assume that the channel matrix can be model as

$$\hat{\mathbf{H}} = \delta \mathbf{H} + (1 - \delta) \Delta \mathbf{H} \quad (28)$$

where $\delta \in [0, 1]$ accounts for the channel estimation factor. $\delta = 0$ implies the case of perfect CSI and $\delta > 0$ means imperfect CSI. Two conditions with different distribution models are considered. 1) *Gaussian model*: the entries of $\Delta \mathbf{H}$ are zero-mean Gaussian distributed, $[\Delta \mathbf{H}]_{ij} \sim \mathcal{CN}(0, 1)$. 2) *Non-Gaussian model*: the entries of $\Delta \mathbf{H}$ follow a uniform distribution, $[\Delta \mathbf{H}]_{ij} \sim \frac{1}{\sqrt{3}} \mathcal{UN}(-1, 1)$.

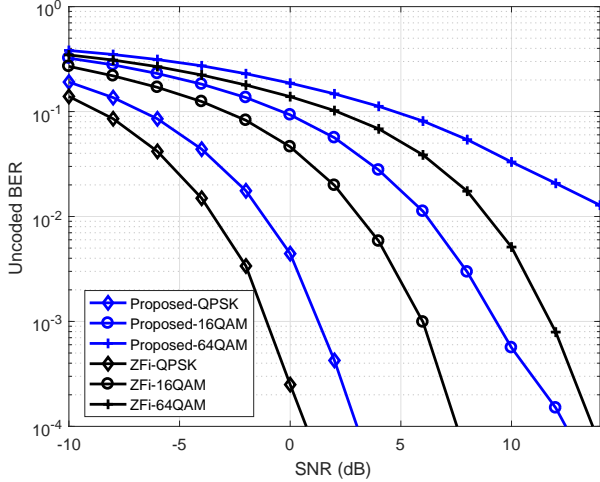


Fig. 6. Performance of the proposed precoder compared with the ideal linear precoder (ZFi) for different modulation modes.

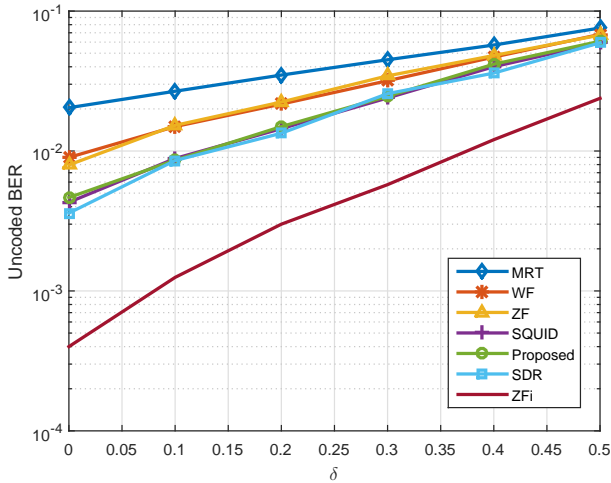


Fig. 7. Un-coded BER of the compared precoders for MU-MIMO with 1-bit DACs in the case of Gaussian channel estimation error (QPSK signaling).

Fig. 7 and Fig. 8 show the performance of the compared precoders versus the strength of the channel estimation error. In the two conditions with QPSK signaling. The SNR is fixed at 0 dB. We consider a MU-MIMO system with 128 BS antennas and 16 UTs. The results indicate that, in both the Gaussian and non-Gaussian error conditions, the nonlinear quantized precoders outperform the linear ones whenever $\delta > 0$. It is demonstrated that, nonlinear quantized precoders can be adopted in the case of imperfect CSI.

VI. CONCLUSIONS

In this paper, we have investigated the nonlinear precoding problem for MU-MIMO downlink systems using 1-bit DACs. We proposed a highly-efficient algorithm based on the ADMM framework to directly solve the nonconvex precoding problem. The proposed algorithm is globally convergent under rather mild conditions. A sufficient condition for its convergence

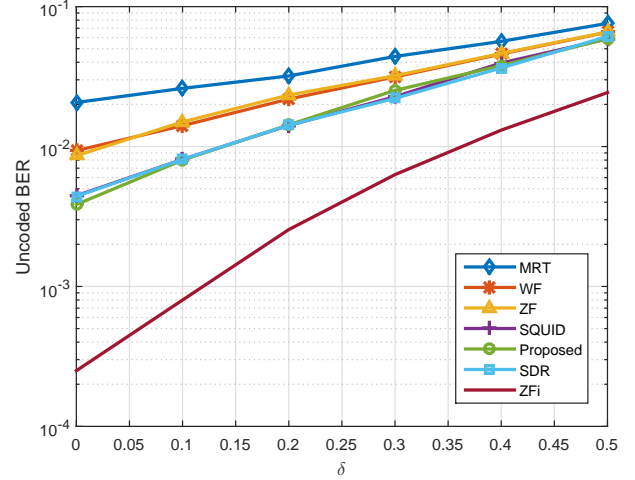


Fig. 8. Un-coded BER of the compared precoders for MU-MIMO with 1-bit DACs in the case of non-Gaussian channel estimation error (QPSK signaling).

has been derived. Finally, various numerical studies have been conducted to verify the effectiveness and efficiency of the new precoder. The results demonstrated that the proposed precoder can achieve state-of-the-art BER performance compared with the SDR precoder. Furthermore, the proposed precoder is the most computationally efficient nonlinear quantized precoder.

Due to the limited space, we leave some works in our future studies. These works include: 1) alleviating the effect of imperfect CSI by powerful tools such as deep learning and random matrix theory; 2) extending the proposed algorithm to the quantized orthogonal frequency division multiplexing (OFDM) MIMO downlink system.

VII. ACKNOWLEDGEMENTS

The authors would like to thank for technical experts: Tian Pan, Guangyi Yang, Rui Gong and Yingzhe Li, all from Huawei Technologies for their fruitful discussions and code reviews.

APPENDIX A PROOF OF LEMMA I

First, the minimizer \mathbf{u}^{k+1} of (18) satisfies

$$\mathcal{L}(\tilde{\mathbf{v}}^k, \mathbf{u}^{k+1}, \mathbf{w}^k) \leq \mathcal{L}(\tilde{\mathbf{v}}^k, \mathbf{u}^k, \mathbf{w}^k). \quad (29)$$

Let $\varphi_1 = \text{eig}_{\min}(\mathbf{H}^T \mathbf{H})$ denote the minimal eigenvalue of $\mathbf{H}^T \mathbf{H}$, it is easy to see that $\mathcal{L}(\tilde{\mathbf{v}}, \mathbf{u}^{k+1}, \mathbf{w}^k)$ is $(2\varphi_1 + 2c + \lambda)$ -strongly convex with respect to $\tilde{\mathbf{v}}$. Thus, for any $\tilde{\mathbf{v}}^k$, the minimizer $\tilde{\mathbf{v}}^{k+1}$ of (19) satisfies

$$\begin{aligned} & \mathcal{L}(\tilde{\mathbf{v}}^{k+1}, \mathbf{u}^{k+1}, \mathbf{w}^k) \\ & \leq \mathcal{L}(\tilde{\mathbf{v}}^k, \mathbf{u}^{k+1}, \mathbf{w}^k) - \frac{2\varphi_1 + 2c + \lambda}{2} \|\tilde{\mathbf{v}}^{k+1} - \tilde{\mathbf{v}}^k\|_2^2. \end{aligned} \quad (30)$$

Moreover, from the definition of \mathcal{L} and with the use of (20), we have

$$\begin{aligned} & \mathcal{L}(\tilde{\mathbf{v}}^{k+1}, \mathbf{u}^{k+1}, \mathbf{w}^{k+1}) - \mathcal{L}(\tilde{\mathbf{v}}^{k+1}, \mathbf{u}^{k+1}, \mathbf{w}^k) \\ & = \frac{1}{\lambda} \|\mathbf{w}^{k+1} - \mathbf{w}^k\|_2^2. \end{aligned} \quad (31)$$

Then, summing (29), (30) and (31) yields

$$\begin{aligned} & \mathcal{L}(\tilde{\mathbf{v}}^{k+1}, \mathbf{u}^{k+1}, \mathbf{w}^{k+1}) - \mathcal{L}(\tilde{\mathbf{v}}^k, \mathbf{u}^k, \mathbf{w}^k) \\ & \leq \frac{1}{\lambda} \|\mathbf{w}^{k+1} - \mathbf{w}^k\|_2^2 - \frac{2\varphi_1 + 2c + \lambda}{2} \|\tilde{\mathbf{v}}^{k+1} - \tilde{\mathbf{v}}^k\|_2^2. \end{aligned} \quad (32)$$

From (19), the minimizer $\tilde{\mathbf{v}}^{k+1}$ given by each iteration satisfies

$$2\mathbf{H}^T(\mathbf{H}\tilde{\mathbf{v}}^{k+1} - \tilde{\mathbf{s}}) + 2c\tilde{\mathbf{v}}^{k+1} + \lambda(\tilde{\mathbf{v}}^{k+1} - \mathbf{u}^{k+1} - \mathbf{w}^k/\lambda) = \mathbf{0}. \quad (33)$$

Substituting (20) into (33) we have

$$2\mathbf{H}^T(\mathbf{H}\tilde{\mathbf{v}}^{k+1} - \tilde{\mathbf{s}}) + 2c\tilde{\mathbf{v}}^{k+1} - \mathbf{w}^{k+1} = \mathbf{0}. \quad (34)$$

Then, we have

$$\begin{aligned} & \|\mathbf{w}^{k+1} - \mathbf{w}^k\|_2^2 \\ & = 4 \|(\mathbf{H}^T\mathbf{H} + c\mathbf{I})(\tilde{\mathbf{v}}^{k+1} - \tilde{\mathbf{v}}^k)\|_2^2, \\ & \leq 4(\varphi_2 + c)^2 \|\tilde{\mathbf{v}}^{k+1} - \tilde{\mathbf{v}}^k\|_2^2 \end{aligned} \quad (35)$$

Consequently, substituting (35) into (32) results in Lemma I.

APPENDIX B PROOF OF LEMMA II

To prove Lemma II, we first show the sequence $\{(\tilde{\mathbf{v}}^k, \mathbf{u}^k, \mathbf{w}^k)\}$ generated via (18)–(20) is bounded if the condition (25) holds. From (34), we have

$$\begin{aligned} \|\mathbf{w}^k\|_2^2 & = 4 \|\mathbf{H}^T(\mathbf{H}\tilde{\mathbf{v}}^k - \tilde{\mathbf{s}}) + c\tilde{\mathbf{v}}^k\|_2^2 \\ & \leq 4(\|\mathbf{H}^T(\mathbf{H}\tilde{\mathbf{v}}^k - \tilde{\mathbf{s}})\|_2 + c\|\tilde{\mathbf{v}}^k\|_2)^2 \\ & \leq 8\|\mathbf{H}^T(\mathbf{H}\tilde{\mathbf{v}}^k - \tilde{\mathbf{s}})\|_2^2 + 8c^2\|\tilde{\mathbf{v}}^k\|_2^2 \\ & \leq 8\varphi_2\|\mathbf{H}\tilde{\mathbf{v}}^k - \tilde{\mathbf{s}}\|_2^2 + 8c^2\|\tilde{\mathbf{v}}^k\|_2^2 \end{aligned} \quad (36)$$

where we have used the relation

$$\varphi_2 = \text{eig}_{\max}(\mathbf{H}^T\mathbf{H}) = \text{eig}_{\max}(\mathbf{H}\mathbf{H}^T).$$

Note that, $\mathcal{L}(\tilde{\mathbf{v}}^k, \mathbf{u}^k, \mathbf{w}^k)$ is bounded from below. When (25) holds, it follows from Lemma I that $\mathcal{L}(\tilde{\mathbf{v}}^k, \mathbf{u}^k, \mathbf{w}^k)$ is non-increasing in the iteration and therefore convergent. Then, from the definition of \mathcal{L} and with the use of (36), for any $k > 1$ we have

$$\begin{aligned} & \mathcal{L}(\tilde{\mathbf{v}}^1, \mathbf{u}^1, \mathbf{w}^1) \\ & \geq \mathcal{L}(\tilde{\mathbf{v}}^k, \mathbf{u}^k, \mathbf{w}^k) \\ & = \left\| \tilde{\mathbf{s}} - \tilde{\mathbf{H}}\tilde{\mathbf{v}}^k \right\|_2^2 + c\|\tilde{\mathbf{v}}^k\|_2^2 + \delta_{\Omega}(\mathbf{u}^k) \\ & \quad + \frac{\lambda}{2} \left\| \tilde{\mathbf{v}}^k - \mathbf{u}^k - \frac{\mathbf{w}^k}{\lambda} \right\|_2^2 - \frac{\|\mathbf{w}^k\|_2^2}{2\lambda} \\ & \geq c_1 \left\| \tilde{\mathbf{s}} - \tilde{\mathbf{H}}\tilde{\mathbf{v}}^k \right\|_2^2 + c_2 \|\tilde{\mathbf{v}}^k\|_2^2 + \delta_{\Omega}(\mathbf{u}^k) \\ & \quad + \frac{\lambda}{2} \left\| \tilde{\mathbf{v}}^k - \mathbf{u}^k - \frac{\mathbf{w}^k}{\lambda} \right\|_2^2 \end{aligned} \quad (37)$$

with $c_1 = 1 - 8\varphi_2/\lambda$ and $c_2 = c - 8c^2/\lambda$. It is easy to see that, when (25) holds, $c_1 > 0$ and $c_2 > 0$, then it follows from (37) that the sequence $\{(\tilde{\mathbf{v}}^k, \mathbf{u}^k, \mathbf{w}^k)\}$ is bounded. Since the sequence $\mathbf{z}^k := (\tilde{\mathbf{v}}^k, \mathbf{u}^k, \mathbf{w}^k)$ is bounded, there exists a convergent subsequence \mathbf{z}^{k_j} that converges to a cluster point \mathbf{z}^* . Meanwhile, from Lemma I, $\mathcal{L}(\mathbf{z}^k)$ is nonincreasing and

convergent when (25) holds, and $\mathcal{L}(\mathbf{z}^k) \geq \mathcal{L}(\mathbf{z}^*)$ for any k . Thus, using the result in Lemma 1 we have

$$\begin{aligned} & \infty > \mathcal{L}(\mathbf{z}^1) - \mathcal{L}(\mathbf{z}^*) \\ & \geq \mathcal{L}(\mathbf{z}^1) - \tilde{\mathcal{L}}(\mathbf{z}^{K+1}) \\ & = \sum_{k=1}^K [\mathcal{L}(\mathbf{z}^k) - \mathcal{L}(\mathbf{z}^{k+1})] \\ & \geq \left[\frac{2\varphi_1 + 2c + \lambda}{2} - \frac{4(\varphi_2 + c)^2}{\lambda} \right] \sum_{k=1}^K \|\tilde{\mathbf{v}}^{k+1} - \tilde{\mathbf{v}}^k\|_2^2. \end{aligned}$$

Let $K \rightarrow \infty$, when (25) holds, we have

$$\frac{2\varphi_1 + 2c + \lambda}{2} - \frac{4(\varphi_2 + c)^2}{\lambda} > 0$$

and it follows that

$$\sum_{k=1}^{\infty} \|\tilde{\mathbf{v}}^{k+1} - \tilde{\mathbf{v}}^k\|_2^2 < \infty \quad (38)$$

which together with (8) and (22) implies

$$\sum_{k=1}^{\infty} \|\mathbf{w}^{k+1} - \mathbf{w}^k\|_2^2 < \infty \quad (39)$$

and

$$\sum_{k=1}^{\infty} \|\mathbf{u}^{k+1} - \mathbf{u}^k\|_2^2 < \infty. \quad (40)$$

Then, from (38), (39), and (40) we have

$$\lim_{k \rightarrow \infty} \|\mathbf{z}^{k+1} - \mathbf{z}^k\|_2^2 = 0.$$

Next, we show that any cluster point of the sequence $\{\mathbf{z}^k\}$ is a stationary point of \mathcal{L} . The sequence generated via the steps (18)–(20) satisfies

$$\begin{cases} \mathbf{0} \in \partial\delta_{\Omega}(\mathbf{u}^{k+1}) + \mathbf{w}^{k+1} + \lambda(\tilde{\mathbf{v}}^{k+1} - \tilde{\mathbf{v}}^k) \\ \mathbf{0} = 2(\mathbf{H}^T\mathbf{H} + c\mathbf{I})\tilde{\mathbf{v}}^{k+1} - 2\mathbf{H}^T\tilde{\mathbf{s}} - \mathbf{w}^{k+1} \\ \mathbf{w}^{k+1} = \mathbf{w}^k - \lambda(\tilde{\mathbf{v}}^{k+1} - \mathbf{u}^{k+1}) \end{cases}. \quad (41)$$

Let $\{\mathbf{z}^{k_j}\}$ denote a convergent subsequence of $\{\mathbf{z}^k\}$, since $\lim_{k \rightarrow \infty} \|\mathbf{z}^{k+1} - \mathbf{z}^k\|_2^2 = 0$, the two sequences $\{\mathbf{z}^{k_j}\}$ and $\{\mathbf{z}^{k_j+1}\}$ have the same limit point, denoted by $\mathbf{z}^* := (\tilde{\mathbf{v}}^*, \mathbf{u}^*, \mathbf{w}^*)$. When the condition (25) is satisfied, $\mathcal{L}(\mathbf{z}^k)$ is convergent, thus $\delta_{\Omega}(\mathbf{u}^{k+1})$ is also convergent. Then, passing to the limit in (41) along the subsequence $\{\mathbf{z}^{k_j}\}$ yields

$$\begin{cases} -\mathbf{w}^* \in \partial\delta_{\Omega}(\mathbf{u}^*) \\ \mathbf{w}^* = 2(\mathbf{H}^T\mathbf{H} + c\mathbf{I})\tilde{\mathbf{v}}^* - 2\mathbf{H}^T\tilde{\mathbf{s}} \\ \tilde{\mathbf{v}}^* = \mathbf{u}^* \end{cases}.$$

Consequently, such a limit point \mathbf{z}^* is a stationary point of the Lagrangian function \mathcal{L} .

APPENDIX C PROOF OF LEMMA III

From the definition of the Lagrangian function in (19), we have

$$\partial_{\mathbf{u}}\mathcal{L}(\mathbf{z}^{k+1}) = \partial\delta_{\Omega}(\mathbf{u}^{k+1}) - (\mathbf{w}^{k+1} - \mathbf{w}^k) + \mathbf{w}^{k+1}$$

which together with the first relation in (41) yields

$$\lambda(\tilde{\mathbf{v}}^{k+1} - \tilde{\mathbf{v}}^k) - (\mathbf{w}^{k+1} - \mathbf{w}^k) \in \partial_{\mathbf{u}} \mathcal{L}(\mathbf{z}^{k+1}).$$

Similarly, we have

$$\partial_{\tilde{\mathbf{v}}} \mathcal{L}(\mathbf{z}^{k+1}) = 2(\mathbf{H}^T \mathbf{H} + c\mathbf{I})\tilde{\mathbf{v}}^{k+1} - 2\mathbf{H}^T \tilde{\mathbf{s}} - \mathbf{w}^k$$

which together with the second relation in (41) implies

$$\partial_{\tilde{\mathbf{v}}} \mathcal{L}(\mathbf{z}^{k+1}) = \mathbf{w}^{k+1} - \mathbf{w}^k.$$

Meanwhile, we have

$$\partial_{\mathbf{w}} \mathcal{L}(\mathbf{z}^{k+1}) = (\mathbf{w}^{k+1} - \mathbf{w}^k)/\lambda.$$

Thus, there exists a constant $c_2 > 0$ such that

$$\text{dist}(0, \partial \mathcal{L}(\mathbf{z}^{k+1})) \leq c_2 \left(\|\tilde{\mathbf{v}}^{k+1} - \tilde{\mathbf{v}}^k\|_2^2 + \|\mathbf{w}^{k+1} - \mathbf{w}^k\|_2^2 \right)$$

which together with (35) results in Lemma III.

APPENDIX D PROOF OF THEOREM I

With the results in Lemma II and Lemma III, the rest proof of Theorem I is to prove that the sequence $\{\mathbf{z}^k\}$ generated by the ADMM algorithm is a *Cauchy sequence* and has finite length

$$\sum_{k=0}^{\infty} \|\mathbf{z}^{k+1} - \mathbf{z}^k\|_2 < \infty.$$

Then, the global convergence of the sequence $\{\mathbf{z}^k\}$ to a stationary point of \mathcal{L} is proved. The derivation of this property relies on the Kurdyka-Lojasiewicz (KL) property of \mathcal{L} . \mathcal{L} is a KL function since it is a composite of an indicator function and analytical function. The rest derivation is omitted here for succinctness since it follows similarly to that in [40] with only some minor changes.

REFERENCES

- [1] L. Liu, R. Chen, S. Geirhofer, K. Sayana, Z. Shi, and Y. Zhou, "Downlink mimo in lte-advanced: Su-mimo vs. mu-mimo," *IEEE Communications Magazine*, vol. 50, no. 2, pp. 140–147, 2012.
- [2] R. Qiu and M. Wicks, *Cognitive Networked Sensing and Big Data*. Springer Publishing Company, Incorporated, 2013.
- [3] F. Rusek, D. Persson, B. K. Lau, and E. G. Larsson, "Scaling up mimo: Opportunities and challenges with very large arrays," *Signal Processing Magazine IEEE*, vol. 30, no. 1, pp. 40–60, 2012.
- [4] M. Joham, W. Utschick, and J. A. Nossek, "Linear transmit processing in mimo communications systems," *IEEE Transactions on Signal Processing*, vol. 53, no. 8, pp. 2700–2712, 2005.
- [5] O. B. Usman, H. Jedda, A. Mezghani, and J. A. Nossek, "Mmse precoder for massive mimo using one-bit quantization," in *IEEE International Conference on Acoustics, Speech and Signal Processing*, 2016, pp. 3381–3385.
- [6] A. Swindlehurst, A. Saxena, A. Mezghani, and I. Fijalkow, "Minimum probability-of-error perturbation precoding for the one-bit massive mimo downlink," in *IEEE International Conference on Acoustics, Speech and Signal Processing*, 2017, pp. 6483–6487.
- [7] J. J. Bussgang, "Crosscorrelation functions of amplitude-distorted gaussian signals," *Bell Lab Technical Report*, vol. Rept. 216, 1952.
- [8] A. Mezghani and J. A. Nossek, "On ultra-wideband mimo systems with one-bit quantized outputs: Performance analysis and input optimization," in *IEEE International Symposium on Information Theory*, 2007, pp. 1286–1289.
- [9] A. B. Ucuncu and A. O. Yilmaz, "Performance analysis of faster than symbol rate sampling in one-bit massive mimo systems," in *IEEE International Conference on Communications*, 2017, pp. 1–6.

- [10] A. Gokceoglu, E. Bjornson, E. G. Larsson, and M. Valkama, "Spatio-temporal waveform design for multi-user massive mimo downlink with one-bit receivers," *IEEE Journal of Selected Topics in Signal Processing*, vol. PP, no. 99, pp. 1–1, 2017.
- [11] A. K. Saxena, I. Fijalkow, and A. L. Swindlehurst, "On one-bit quantized zf precoding for the multiuser massive mimo downlink," in *Sensor Array and Multichannel Signal Processing Workshop*, 2016.
- [12] S. Jacobsson, G. Durisi, M. Coldrey, and C. Studer, "Massive mu-mimo-ofdm downlink with 1-bit dacs and linear precoding," in *GLOBECOM 2017 - 2017 IEEE Global Communications Conference*, 2017, pp. 1–6.
- [13] O. B. Usman, J. A. Nossek, C. A. Hofmann, and A. Knopp, "Joint mmse precoder and equalizer for massive mimo using one-bit quantization," in *IEEE International Conference on Communications*, 2017, pp. 1–6.
- [14] H. Yang, G. Geraci, T. Q. S. Quek, and J. Andrews, "Cell-edge-aware precoding for downlink massive mimo cellular networks," *IEEE Transactions on Signal Processing*, vol. PP, no. 99, pp. 1–1, 2017.
- [15] J. Guerreiro, R. Dinis, and P. Montezuma, "Use of one-bit digital-to-analogue converters in massive mimo systems," *Electronics Letters*, vol. 52, no. 9, pp. 778–779, 2016.
- [16] A. K. Saxena, I. Fijalkow, and A. L. Swindlehurst, "Analysis of 1-bit quantized precoding for the multiuser massive mimo downlink," *IEEE Transactions on Signal Processing*, vol. 65, no. 17, pp. 4624–4634, 2017.
- [17] H. Jedda, A. Mezghani, J. A. Nossek, and A. L. Swindlehurst, "Massive mimo downlink one-bit precoding with linear programming for psk signaling," in *IEEE International Workshop on Signal Processing Advances in Wireless Communications*, 2017, pp. 1–5.
- [18] J. Xu, W. Xu, and F. Gong, "On performance of quantized transceiver in multiuser massive mimo downlinks," *IEEE Wireless Communications Letters*, vol. PP, no. 99, pp. 1–1, 2017.
- [19] O. Castaneda, S. Jacobsson, G. Durisi, M. Coldrey, T. Goldstein, and C. Studer, "one-bit massive mu-mimo precoding in vlsi," *IEEE Journal on Emerging and Selected Topics in Circuits and Systems*, vol. PP, no. 99, pp. 1–1, 2017.
- [20] Y. Li, C. Tao, A. L. Swindlehurst, A. Mezghani, and L. Liu, "Downlink achievable rate analysis in massive mimo systems with 1-bit dacs," *IEEE Communications Letters*, vol. 21, no. 7, pp. 1669–1672, 2017.
- [21] H. Jedda, J. A. Nossek, and A. Mezghani, "Minimum ber precoding in 1-bit massive mimo systems," in *Sensor Array and Multichannel Signal Processing Workshop*, 2016.
- [22] S. Jacobsson, G. Durisi, M. Coldrey, T. Goldstein, and C. Studer, "Quantized precoding for massive mu-mimo," *IEEE Transactions on Communications*, vol. 65, no. 11, pp. 4670 – 4684, 2017.
- [23] O. Castaneda, T. Goldstein, and C. Studer, "Pokemon: A non-linear beamforming algorithm for one-bit massive mimo," in *IEEE International Conference on Acoustics, Speech and Signal Processing*, 2017, pp. 3464–3468.
- [24] S. Jacobsson, G. Durisi, M. Coldrey, T. Goldstein, and C. Studer, "Nonlinear one-bit precoding for massive mu-mimo with higher-order modulation," in *2016 50th Asilomar Conference on Signals, Systems and Computers*, 2016, pp. 763–767.
- [25] D. W. K. Ng, E. S. Lo, and R. Schober, "Robust beamforming for secure communication in systems with wireless information and power transfer," *IEEE Transactions on Wireless Communications*, vol. 13, no. 8, pp. 4599–4615, 2014.
- [26] T. L. Marzetta, "Noncooperative cellular wireless with unlimited numbers of base station antennas," *IEEE Transactions on Wireless Communications*, vol. 9, no. 11, pp. 3590–3600, 2010.
- [27] Y. H. Nam, B. L. Ng, K. Sayana, and Y. Li, "Full-dimension mimo (fd-mimo) for next generation cellular technology," *IEEE Communications Magazine*, vol. 51, no. 6, pp. 172–179, 2013.
- [28] J. Jose, A. Ashikhmin, T. L. Marzetta, and S. Vishwanath, "Pilot contamination and precoding in multi-cell tdd systems," *IEEE Transactions on Wireless Communications*, vol. 10, no. 8, pp. 2640–2651, 2011.
- [29] A. Goldsmith, *Wireless communications*. Cambridge: Cambridge Univ. Press, 2005.
- [30] B. M. Hochwald, C. B. Peel, and A. L. Swindlehurst, "A vector-perturbation technique for near-capacity multiantenna multiuser communication-part ii: perturbation," *IEEE Transactions on Communications*, vol. 53, no. 3, pp. 537–544, 2005.
- [31] E. Agrell, T. Eriksson, A. Vardy, and K. Zeger, "Closest point search in lattices," *IEEE Transactions on Information Theory*, vol. 48, no. 8, pp. 2201–2214, 2002.
- [32] J. Jalden and B. Ottersten, "On the complexity of sphere decoding in digital communications," *IEEE Transactions on Signal Processing*, vol. 53, no. 4, pp. 1474–1484, 2005.

- [33] N. D. Sidiropoulos and Z. Q. Luo, "A semidefinite relaxation approach to mimo detection for high-order qam constellations," *IEEE Signal Processing Letters*, vol. 13, no. 9, pp. 525–528, 2006.
- [34] M. Kisialiou and Z.-Q. Luo, "Probabilistic analysis of semidefinite relaxation for binary quadratic minimization," *SIAM J. on Optimization*, vol. 20, no. 4, pp. 1906–1922, 2010.
- [35] Boyd, Vandenberghe, and Foybusovich, "Convex optimization," *IEEE Transactions on Automatic Control*, vol. 51, no. 11, pp. 1859–1859, 2006.
- [36] Z. Q. Luo, W. K. Ma, M. C. So, Y. Ye, and S. Zhang, "Semidefinite relaxation of quadratic optimization problems," *IEEE Signal Processing Magazine*, vol. 27, no. 3, pp. 20–34, 2010.
- [37] F. Wen, P. Liu, Y. Liu, R. C. Qiu, and W. Yu, "Robust sparse recovery in impulsive noise via lp-11 optimization," *IEEE Transactions on Signal Processing*, vol. 65, no. 1, pp. 105–118, 2017.
- [38] F. Wen, L. Adhikari, L. Pei, R. Marcia, P. Liu, and R. Qiu, "Nonconvex regularization based sparse recovery and demixing with application to color image inpainting," *IEEE Access*, vol. PP, no. 99, pp. 1–1, 2017.
- [39] F. Wen, L. Pei, Y. Yang, W. Yu, and P. Liu, "Efficient and robust recovery of sparse signal and image using generalized nonconvex regularization," *IEEE Transactions on Computational Imaging*, vol. PP, no. 99, pp. 1–1, 2017.
- [40] G. Li and T. K. Pong, "Global convergence of splitting methods for nonconvex composite optimization," *SIAM Journal on Optimization*, vol. 25, no. 4, pp. 2434–2460, 2015.
- [41] Y. Hu, D. Zhang, J. Ye, X. Li, and X. He, "Fast and accurate matrix completion via truncated nuclear norm regularization," *IEEE Transactions on Pattern Analysis and Machine Intelligence*, vol. 35, no. 9, pp. 2117–2130, 2013.